Structural and Spectroscopic Studies of 16-Electron, Unsaturated Derivatives of Low-Valent, Group 6 Carbonyl Complexes Containing π-Donor Ligands

Donald J. Darensbourg,* Jennifer D. Draper, Brian J. Frost, and Joseph H. Reibenspies

Department of Chemistry, Texas A&M University, P.O. Box 30012, College Station, Texas 77842

Received April 13, 1998

Several eighteen- and sixteen-electron derivatives of tungsten(0), molybdenum(0), and chromium(0) carbonyl complexes, including $[PPN]_2[Cr(CO)_3(O,S\text{-}C_6H_4)]$ (**2c**), $[PPN]_2[W(CO)_3(NH,S\text{-}C_6H_4)]$ (**5c**), $[PPN]_2[W(CO)_3(O,S\text{-}C_6H_4)]$ (**6c**), $[PPN]_2[W(CO)_4(S,S\text{-}C_6H_4)]$ (**7b**) have been synthesized from the reaction of photochemically generated $M(CO)_5THF$ with a series of doubly deprotonated 1,2-disubstituted benzene rings with the appropriate oxygen, nitrogen, and sulfur donor atoms. These complexes have been characterized in the solid state by X-ray crystallography and in solution by IR and ^{13}C NMR spectroscopies. The crystal of **2c** ($C_{84}H_{71}N_3O_5P_4SCr$) is triclinic $P\bar{1}$, a =13.869(3) Å, b = 23.128(5) Å, c = 12.056(2) Å, α = 104.84(3)°, β = 106.91(3)°, γ = 95.29(3)°, Z = 2; that of **5c** ($C_{89}H_{77}N_7O_3P_4SW$) is monoclinic $P2_1$, a = 11.054(2) Å, b = 28.140(6) Å, c = 12.566(2) Å, β = 90.58(1)°, Z = 2; that of **6c** ($C_{85}H_{70}N_4O_4P_4SW$) is triclinic $P\bar{1}$, 12.236(2) Å, b = 14.419(2) Å, c = 22.748(4) Å, α = 76.44(1)°, β = 75.98(2)°, γ = 70.98(1)°, Z = 2; that of **7b** ($C_{82}H_{64}N_2O_4P_4S_2W$) is triclinic $P\bar{1}$, a = 12.650(1) Å, b = 14.810(1) Å, c = 21.053(2) Å, α = 77.182(7)°, β = 78.334(7)°, γ = 66.579(7), Z = 2; and that of **8** ($C_{10}H_8O_4P_2W$) is monoclinic $P2_1/c$, a = 11.582(1) Å, b = 10.791(1) Å, c = 10.449(1) Å, β = 100.867(7)°, Z = 2. The average ν(CO) frequencies for each tricarbonyl species reported are compared to those related dianions previously reported in order to gauge the π-donor character of the different ligands. The ^{13}C NMR spectrum for each tricarbonyl derivative consists of a single sharp peak for the three inequivalent carbonyls as a result of a low-energy, fast intramolecular exchange process. Both inter- and intramolecular CO-exchange processes have been probed via variable temperature ^{13}C NMR. In the case of the 16-electron species the geometry of the metal dianion is that of a distorted trigonal bipyramid consisting of three carbonyl ligands and a five-membered chelate ring bound through the π-donor atoms at an equatorial and an axial position, with the stronger π-donor atom in the equatorial site. The equatorial site for the most effective π-donor is preferred over the axial position because the unoccupied d_{xy} orbital lies in the equatorial plane, and may be stabilized via a π-donor ligand in the equatorial position. The axial position exhibits a filled/filled repulsion as both orbitals available for π-bonding are filled.

Introduction

The dissociative mechanism that affords an intermediate of reduced coordination number, is by far the most common pathway for substitution reactions involving 18-electron metal carbonyl derivatives. It has been well established that ancillary ligands capable of π-donation can stabilize these coordinatively unsaturated intermediates generated in ligand substitution reactions.[1,2] This stabilization due to π-donation may have two outcomes: (i) the rate of exchange increases in proportion to the degree of stabilization imparted by the π-donor (D) to result in product **B** (Scheme 1)[3] or (ii) the π-donation is sufficient to stabilize the unsaturated intermediate, **A**; i.e., the intermediate is stabilized to the extent that the formation of a M−X bond is either thermodynamically unfavorable or only slightly favorable such that **A** is isolable.[4−8]

Scheme 1

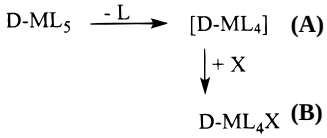

Over the last several years, considerable efforts have been directed into understanding the nature of π-donor ligands as they relate to **A** and **B** above. That is, what are the properties of π-donor ligands that cause **B** to be favored over **A**? Pursuant to answering these questions the synthesis and structural characterizations of several group 6 zerovalent unsaturated carbonyl species consistent with **A** (Scheme 1) have been published.[7−11]

In previous studies the exclusive use of ligands containing oxygen and nitrogen donor atoms, both exceptional π-donors, limited the ability to examine the equilibrium between **A** and

(1) Cotton, F. A.; Wilkinson, G. *Advanced Inorganic Chemistry*, 5th ed.; John Wiley & Sons: New York, 1988.
(2) Basolo, F.; Pearson, R. G. *Mechanisms of Inorganic Reactions*, 2nd ed.; Wiley and Sons: New York, 1967.
(3) Darensbourg, D. J.; Sanchez, K. M.; Reibenspies, J. H.; Rheingold, A. L. *J. Am. Chem. Soc.* **1989**, *111*, 7094.
(4) Lunder, D. M.; Lobkovsky, E. B.; Streib, W. E.; Caulton, K. G. *J. Am. Chem. Soc.* **1991**, *113*, 1837.
(5) Ashby, M. T.; Enemark, J. H. *J. Am. Chem. Soc.* **1986**, *108*, 730.
(6) Hubbard, J. L.; McVicar, W. K. *Inorg. Chem.* **1992**, *31*, 910.
(7) Sellmann, D.; Wilke, M.; Knoch, F. *Inorg. Chem.* **1993**, *32*, 2534.
(8) Sellmann, D.; Ludwig, W.; Huttner, G.; Zsolnai, L. *J. Organomet.* **1985**, *294*, 199.
(9) Darensbourg, D. J.; Klausmeyer, K. K.; Mueller, B. C.; Reibenspies, J. H. *Angew. Chem., Int. Ed. Engl.* **1992**, *31*, 1503.
(10) Darensbourg, D. J.; Klausmeyer, K. K.; Reibenspies, J. H. *Inorg. Chem.* **1996**, *35*, 1529.
(11) Darensbourg, D. J.; Klausmeyer, K. K.; Reibenspies, J. H. *Inorg. Chem.* **1996**, *35*, 1535.

10.1021/ic9804216 CCC: $18.00
Published on Web 09/23/1999

B by favoring the formation of the 16-electron product. Specifically of interest now is eq 1, where M = Cr(0), Mo(0), or W(0), and X and Y are π-donor atoms appended to the phenyl ring.

$$M(CO)_4(X,Y\text{-}C_6H_4)^{2-} \underset{+CO}{\overset{-CO}{\rightleftharpoons}} M(CO)_3(X,Y\text{-}C_6H_4)^{2-} \quad (1)$$

A number of 1,2-disubstituted benzene rings with varying O, N, S, and P donor atoms were selected to function as the ancillary potentially π-donating ligands. The purpose served here is 2-fold: (i) the π-donating ability of sulfur and phosphorus are significantly weaker than that of nitrogen and oxygen,[12,13] increasing the chances of observing the exchange dynamics between the tetracarbonyl and tricarbonyl derivatives in eq 1 and (ii) the interactions of atoms with significantly diverse π-donor qualities, i.e., nitrogen and sulfur, that generate an unsaturated species are of interest.

Herein, the synthesis and characterization, both spectroscopic and crystallographic, of several new group 6 low-valent tricarbonyl derivatives, are presented. In addition, spectroscopic data relevant to the tetracarbonyl analogues of the unsaturated species has been gathered. Infrared and variable temperature ^{13}C NMR studies that divulge the state of the equilibrium between the saturated vs the unsaturated species in solution will be presented. Finally, these findings will be compared and contrasted with results published previously, as well as compared to computations performed on a series of these complexes. Overall conclusions regarding the nature of π-donor ligands will be discussed.

Experimental Section

Methods and Materials. All manipulations were performed on a double-manifold Schlenk vacuum line under an atmosphere of argon or in an argon-filled glovebox. Solvents were dried and deoxygenated by distillation from the appropriate reagent under a nitrogen atmosphere. Photolysis experiments were performed using a mercury arc 450W UV immersion lamp purchased from Ace Glass Co. Infrared spectra were recorded on a Mattson 6022 spectrometer with DTGS and MCT detectors. Routine infrared spectra were collected using a 0.10-mm CaF_2 cell. ^{13}C NMR spectra were obtained on a Varian XL-200 spectrometer. ^{13}CO was purchased from Cambridge Isotopes and used as received. $Cr(CO)_6$ and $W(CO)_6$ were purchased from Strem Chemicals, Inc., and used without further purification. Sodium methoxide, bis(triphenylphosphoranylidiene)ammonium chloride (PPNCl), $Mo(CO)_6$, 2-aminothiophenol (NH_2,SH-C_6H_4), and 1,2-dithiobenzene (SH,SH-C_6H_4) were purchased from Aldrich. 2-Hydroxythiophenol (OH,SH-C_6H_4) was purchased from Lancaster Synthesis; 1,2-diphosphinobenzene (PH_2,PH_2-C_6H_4) was purchased from Strem Chemicals. $W(CO)_4$(piperidine)$_2$ was prepared by the literature method cited.[14] Microanalyses were performed by Canadian Microanalytical Service, Ltd., Delta, B.C.

Synthesis of [PPN][HX] [X = (O,S-C_6H_4)$^{2-}$, (NH,S-C_6H_4)$^{2-}$, or dtb (S,S-C_6H_4)$^{2-}$] Salts. The synthesis of these salts was accomplished in greater than 90% yield by the slow addition of 1 equiv (1.4 mmol) each of NaOMe and PPNCl in 10 mL of a 1:1 solvent mix of CH_3CN and CH_3OH to 20 mL of a clear [X = (O,S-C_6H_4)$^{2-}$] or yellow [X = (NH,S-C_6H_4)$^{2-}$ or (S,S-C_6H_4)$^{2-}$] solution of the appropriate ligand in CH_3CN. This mixture was stirred for 60 min at ambient temperature and the solvent was removed by vacuum overnight, yielding an off-white [X = (O,S-C_6H_4)$^{2-}$] or bright yellow [X = (NH,S-C_6H_4)$^{2-}$ or (S,S-C_6H_4)$^{2-}$] powder.

Synthesis of [PPN][M(CO)$_5$(HX)] Derivatives (1a−7a). The synthesis of [PPN][M(CO)$_5$HX] [M = W, Mo, or Cr; X = (NH,S-C_6H_4)$^{2-}$,(O,S-C_6H_4)$^{2-}$, or (S,S-C_6H_4)$^{2-}$] was accomplished in yields in excess of 80% by the reaction of 1 equiv of M(CO)$_5$THF (prepared by the photolysis of 0.300 g of $Cr(CO)_6$, 0.400 g of $Mo(CO)_6$, or 0.500 g of $W(CO)_6$ in THF) with 1 equiv (1.4 mmol) of the appropriate deprotonated ligand at ambient temperature.

Synthesis of [PPN]$_2$[M(CO)$_4$(X)] Derivatives (1b−7b). The synthesis of [PPN]$_2$[M(CO)$_4$(X)] was accomplished by the slow addition of a second equivalent (1.4 mmol) of NaOMe and PPNCl, dissolved in 5 mL in a 1:1 CH_3CN/CH_3OH, to the THF solution of the pentacarbonyl derivative (**1a**−**7a**) to yield a dark red solution. The M(CO)$_5$THF intermediates were identified by their ν(CO) infrared spectra: M = Cr, 2073 (w), 1936 (s), 1894 (m); M = W, 2073(w), 1929 (s), 1890 (m) cm^{-1}. Longer photolysis times for $W(CO)_6$ will lead to production of *cis*-$W(CO)_4(THF)_2$, ν(CO): 2013 (w), 1876 (vs), 1830 (m) cm^{-1}. The mixture was allowed to stir 60 min after which the solvent was removed via vacuum overnight. The resulting dark red powder was dissolved in CH_3CN, filtered through Celite to remove the insoluble NaCl and washed several times with 10 mL portions of hexanes to remove any residual $M(CO)_6$. Anal. Calcd for [PPN]$_2$[Cr(CO)$_4$(NH,S-C_6H_4)] (**1b**) ($C_{82}H_{65}N_3O_4P_4SCr$): C, 72.19; H, 4.80; N, 3.08. Found C, 71.92; H, 4.75; N, 2.98. [PPN]$_2$[Cr(CO)$_4$(O,S-C_6H_4)] (**2b**) ($C_{82}H_{64}N_2O_5P_4SCr$): C, 72.13; H, 4.72; N, 2.05. Found: C, 71.30; H, 4.54; N, 1.93. [PPN]$_2$[Mo(CO)$_4$(O,S-C_6H_4)] (**4b**) ($C_{82}H_{64}N_2O_5P_4SMo$): C, 69.89; H, 4.58; N, 1.99. Found: C, 68.93; H, 4.35; N, 2.03. [PPN]$_2$[W(CO)$_4$(O,S-C_6H_4)] (**6b**) ($C_{82}H_{64}N_2O_5P_4SW$): C, 65.78; H, 4.31; N, 1.87. Found: C, 65.32; H, 4.24; N, 1.82. [PPN]$_2$[W(CO)$_4$(S,S-C_6H_4)] (**7b**) ($C_{82}H_{64}N_2O_4P_4S_2W$): C, 65.08; H, 4.26; N, 1.85. Found: C, 64.04; H, 4.24; N, 1.89.

Synthesis of [PPN]$_2$[M(CO)$_3$(X)] Derivatives (1c−7c). The synthesis of the unsaturated, 16-electron tricarbonyl derivative was accomplished by bubbling Argon through a gently heated (40 °C) CH_3CN solution of the tetracarbonyl derivative. Because of their extreme air-sensitivity, and because of their propensity to exist as a mixture of tetra- and tricarbonyl species, elemental analyses were in general not obtained for complexes **1c**−**7c**. However, infrared spectroscopy studies in the υ(CO) region carried out on the crystals of **1c**, **5c**, and **6c** offered spectra that match that of the bulk sample. Furthermore, it was possible to obtain satisfactory elemental analysis for **6c** which crystallized with two molecules of acetonitrile in the lattice. Anal. Calcd for [PPN]$_2$[W(CO)$_3$(O,S-C_6H_4)]·2CH_3CN ($C_{85}H_{70}N_4O_4P_4SW$): C, 65.81; H, 4.55; N, 3.61. Found: C, 65.02; H, 4.38; N, 3.54.

Synthesis of W(CO)$_4$($PH_2C_6H_4PH_2$), 8. The synthesis of W(CO)$_4$($PH_2C_6H_4PH_2$) was accomplished in 75% yield by the reaction of 0.10 g (0.704 mmol) of diphosphinobenzene (^{31}P NMR (CD_3CN) δ −124.6 ppm) with 1 equiv of $W(CO)_4$(piperidine)$_2$ [IR, ν(CO): THF, 2002.0 (w), 1860.2 (vs), 1824.6 (m)] at 40 °C in THF for 2 h. The solvent and free piperidine were removed via vacuum to yield a light brown powder. IR, ν(CO): CH_3CN, 2033.8 (w), 1944.1 (w), 1924.8 (vs) (in CH_3CN). ^{31}P NMR (CD_3CN) δ −62.4 ppm, $^1J_{W-P}$ = 212.3 Hz. Anal. Calcd for W(CO)$_4$(PH_2,PH_2-C_6H_4) (**8**) ($C_{10}H_8O_4P_2W$): C, 27.42; H, 1.84; O, 14.60. Found: C, 27.26; H, 1.74; O, 14.19. Attempts to doubly deprotonate **8** via NaH, NaOMe, *n*-butyllithium, or Et_4NOH were carried out by the slow, stepwise addition of 2 equiv of the appropriate reagent to a dilute solution of **8** in CH_3CN, resulting in the formation of a bright yellow product which decomposed rapidly to a dark brown solution.

X-ray Crystallography of [PPN]$_2$[M(CO)$_3$(X)] Derivatives (2c, 5c, and 6c) [M = Cr, X = (O,S-C_6H_4)$^{2-}$ (1c), M = W, X = (NH,S-C_6H_4)$^{2-}$ (5c), M = W, X = (O,S-C_6H_4)$^{2-}$ (6c)]. Crystal data and details of data collection are given in Table 1. A bright red block of **2c**, a medium red block of **5c**, and a dark-red block of **6c** were mounted on glass fibers with epoxy cement at room temperature and cooled to 193 K in a liquid nitrogen cold stream. Preliminary examination and data collection were performed on a Rigaku AFC5R X-ray diffractometer (Cu Kα, λ = 1.541 78) for **2c** and a Siemens P4 X-ray diffractometer (Mo Kα, λ = 0.710 73 Å radiation) for **5c** and **6c**. Cell parameters were calculated from the least-squares fitting of the setting angles for 24 reflections.

Omega scans for several intense reflections indicated acceptable crystal quality. Data were collected for $4.0° \geq 2\theta \geq 50°$. Three control reflections, collected for every 97 reflections, showed no significant

(12) Poulton, J. T.; Folting, K.; Streib, W. E.; Caulton, K. G. *Inorg. Chem.* **1992**, *31*, 3191.
(13) Poulton, J. T.; Sigalas, M. P.; Folting, K.; Streib, W. E.; Eisenstein, O.; Caulton, K. G. *Inorg. Chem.* **1994**, *33*, 1476.
(14) Darensbourg, D. J.; Kump, R. L. *Inorg. Chem.* **1978**, *17*, 2680.

Table 1. Crystallographic Data for Complexes **2c**, **5c**, **6c**, **7b**, and **8**

	2c	**5c**	**6c**	**7b**	**8**
empirical formula	$C_{84}H_{71}N_3O_5P_4SCr$	$C_{89}H_{77}N_7O_3P_4SW$	$C_{85}H_{70}N_4O_4P_4SW$	$C_{82}H_{64}N_2O_4P_4S_2W$	$C_{10}H_8O_4P_2W$
fw	1410.35	1629.5	1549.5	1511.5	438.0
space group	$P\bar{1}$	$P2_1$	$P\bar{1}$	$P\bar{1}$	$P2_1/c$
V, Å^3	3517.5(1)	3908.6(1)	3628.0(1)	3500.0(5)	1282.5(2)
Z	2	2	2	2	2
d_{calc}, g/cm^3	1.329	1.384	1.418	1.434	1.134
a, Å	13.869(3)	11.054(2)	12.236(2)	12.650(1)	11.582(1)
b, Å	23.128(5)	28.140(6)	14.419(2)	14.810(1)	10.791(1)
c, Å	12.056(2)	12.566(2)	22.748(4)	21.053(2)	10.449(1)
α, deg	104.84(3)	−	76.44(1)	77.182(7)	−
β, deg	106.91(3)	90.58(1)	75.98(2)	78.334(7)	100.867(7)
γ, deg	95.29(3)	−	70.98(1)	66.579(7)	−
T, K	193	193	193	193	193
μ(Mo Kα), mm^{-1}	0.340	3.283	1.764	1.855	9.254
wavelength, Å	0.710 73	0.710 73	0.710 73	0.710 73	0.710 73
R_F,[a] %	8.15	3.62	7.13	3.46	4.27
R_{wF},[b] %	18.78	8.54	13.57	8.19	10.64

[a] $R_F = \sum|F_o - F_c|/\sum F_o$. [b] $R_{wF} = \{[\sum w(F_o^2 - F_c^2)^2]/(\sum wF_o^2)\}^{1/2}$.

Scheme 2[a]

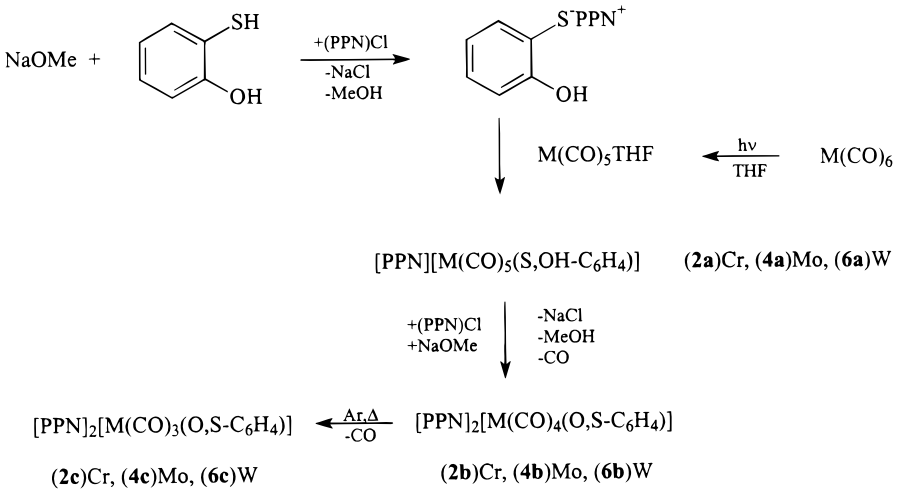

[a] For S,NH_2-$C_6H_4^-$, **1a** = Cr, **3a** = Mo, and **5a** = W; for S,SH-$C_6H_4^-$, **7a** = W.

trends. Background measurements by stationary-crystal and stationary-counter techniques were taken at the beginning and end of each scan for half the total scan time. Lorentz and polarization corrections were applied to 9174 reflections for **2c**, 7017 for **5c**, and 12743 for **6c**. A semiempirical absorption correction was applied to **2c** and **6c**. A total of 9151 unique reflections for **2c**, 7007 for **5c**, and 12 730 for **6c**, with $|I| \geq 2.0\sigma(I)$, were used in further calculations. All three structures were solved by direct methods [SHELXS program package, Sheldrick (1993)]. Full-matrix least-squares anisotropic refinement for all non-hydrogen atoms yielded $R = 0.0815$, $R_w = 0.1878$, and $S = 1.003$ for **2c**, $R = 0.0854$, $R_w = 0.0362$, and $S = 1.051$ for **5c**, and $R = 0.0713$, $R_w = 0.1357$, and $S = 1.017$ for **6c**. Hydrogen atoms were placed in idealized positions with isotropic thermal parameters fixed at 0.08. Neutral-atom scattering factors and anomalous scattering correction terms were taken from *International Tables for X-ray Crystallography*.

X-ray Crystallography of $[PPN]_2[W(CO)_4(S,S\text{-}C_6H_4)]$, 7b. Crystal data and details of data collection are given in Table 1. A red block of **7b** was mounted on a glass fiber with epoxy cement at room temperature and cooled in a liquid nitrogen cold stream. Preliminary examination and data collection were performed on a Siemens P4 X-ray diffractometer (Mo Kα, $\lambda = 0.710\ 73$). Data collection methods and parameters are identical to that described for complexes **2c, 5c**, and **6c**. Lorentz and polarization corrections were applied to 12 257 reflections for **7b**. A semiempirical absorption correction was applied to **7b**. A total of 12 257 unique reflections were used in further calculations. Anisotropic refinement for all non-hydrogen atoms yielded $R = 0.0346$, $R_w = 0.0819$, and $S = 1.070$.

X-ray Crystallography of $[W(CO)_4(PH_2,PH_2\text{-}C_6H_4)]$, 8. Crystal data and details of data collection are given in Table 1. A beige block of **8** was mounted on a glass fiber with epoxy cement at room temperature and cooled in a liquid nitrogen cold stream. Preliminary examination and data collection were performed on a Siemens P4 X-ray diffractometer (Mo Kα, $\lambda = 0.710\ 73$). Data collection methods and parameters are identical to that described for complexes **2c**, **5c**, and **6c**. Lorentz and polarization corrections were applied to 2254 reflections for **8**. A total of 2254 unique reflections were used in further calculations. Anisotropic refinement for all non-hydrogen atoms yielded $R = 0.0427$, $R_w = 0.1064$, and $S = 1.026$.

Computational Details. Theoretical calculations were carried out on a series of $[M(CO)_4(X,Y\text{-}C_6H_4)]^{2-}$/$[M(CO)_3(X,Y\text{-}C_6H_4)]^{2-}$ systems where M = W, Cr; X = N, O, S; Y = N, O, S. All calculations were performed using Gaussian 94[15] running on a SGI power challenge. Geometry optimizations were performed starting from crystal structures where possible and modifications of existing structures when no structure was readily available. Geometry optimizations were performed on all complexes at the Hartree−Fock (HF) level using the LANL2DZ

(15) Frisch, M. J.; Trucks, G. W.; Schlegel, H. B.; Gill, P. M. W.; Johnson, B. G.; Robb, M. A.; Cheeseman, J. R.; Keith, T.; Petersson, G. A.; Montgomery, J. A.; Raghavachari, K.; Al-Laham, M. A.; Zakrzewski, V. G.; Ortiz, J. V.; Foresman, J. B.; Cioslowski, J.; Stefanov, B. B.; Nanayakkara, A.; Challacombe, M.; Peng, C. Y.; Ayala, P. Y.; Chen, W.; Wong, M. W.; Andres, J. L.; Replogle, E. S.; Gomperts, R.; Martin, R. L.; Fox, D. J.; Binkley, J. S.; Defrees, D. J.: Baker, J.; Stewart, J. P.; Head-Gordon, M.; Gonzalez, C.; and Pople, J. A. *GAUSSIAN 94*, Rev. D.4; Gaussian, Inc.: Pittsburgh, PA, 1995.

Table 2. Carbonyl Stretching Frequencies of $[M(CO)_5(HX)]^-$ and $[M(CO)_{4,3}(X)]^{2-}$ Derivatives

complex[a]		ν(C≡O), cm^{-1}				av ν(C≡O), cm^{-1}
$Cr(CO)_5(S,NH_2\text{-}C_6H_4)^-$	**1a**	2044.4(w)	1916.2(s)	1857.3(m)[b]	–	1939
$Cr(CO)_5(S,OH\text{-}C_6H_4)^-$	**2a**	2045.4(w)	1916.2(s)	1853.8(m)[b]	–	1939
$Mo(CO)_5(S,NH_2\text{-}C_6H_4)^-$	**3a**	2053.1(w)	1921.0(s)	1854.4(m)[b]	–	1943
$Mo(CO)_5(S,OH\text{-}C_6H_4)^-$	**4a**	2057.0(w)	1922.9(s)	1861.2(m)[b]	–	1947
$W(CO)_5(S,NH_2\text{-}C_6H_4)^-$	**5a**	2052.1(w)	1911.3(s)	1853.5(m)[b]	–	1939
$W(CO)_5(S,OH\text{-}C_6H_4)^-$	**6a**	2056.0(w)	1915.2(s)	1857.3(m)[b]	–	1943
$W(CO)_5(S,SH\text{-}C_6H_4)^-$	**7a**	2061.3(w)	1919.8(s)	1860.6(m)[b]	–	1947
$Cr(CO)_4(NH,S\text{-}C_6H_4)^{2-}$	**1b**	1989.5(w)	1877.6(vs)	1876.6(sh)	1811.1(m)[c]	1889
$Cr(CO)_4(O,S\text{-}C_6H_4)^{2-}$	**2b**	1991.4(w)	1849.6(vs)	1815.9(sh)	1761.9(m)[c]	1856
$Mo(CO)_4(NH,S\text{-}C_6H_4)^{2-}$	**3b**	1984.6(w)	1862.2(vs)	1821.7(sh)	1797.6(m)[c]	1866
$Mo(CO)_4(O,S\text{-}C_6H_4)^{2-}$	**4b**	1980.8(w)	1850.6(vs)	1814.9(sh)	1766.7(m)[c]	1853
$W(CO)_4(NH,S\text{-}C_6H_4)^{2-}$	**5b**	1992.3(w)	1857.5(vs)	1839(sh)	1792.7(m)[c]	1870
$W(CO)_4(O,S\text{-}C_6H_4)^{2-}$	**6b**	1971.1(w)	1834.2(vs)	1808(sh)	1762.8(m)[c]	1844
$W(CO)_4(S,S\text{-}C_6H_4)^{2-}$	**7b**	1976.9(w)	1845.8(s)	1810.1(sh)	1765.7(m)[c]	1850
$Cr(CO)_3(NH,S\text{-}C_6H_4)^{2-}$	**1c**	1857.3(m)	1726.2(s)[c]	–	–	1792
$Cr(CO)_3(O,S\text{-}C_6H_4)^{2-}$	**2c**	1871.8(m)	1737.8(s)[c]	–	–	1805
$Mo(CO)_3(NH,S\text{-}C_6H_4)^{2-}$	**3c**	1866.0(m)	1739.7(s)[c]	–	–	1802
$Mo(CO)_3(O,S\text{-}C_6H_4)^{2-}$	**4c**	1875.7(m)	1741.6(s)[c]	–	–	1808
$W(CO)_3(NH,S\text{-}C_6H_4)^{2-}$	**5c**	1853.5(m)	1724.3(s)[c]	–	–	1789
$W(CO)_3(O,S\text{-}C_6H_4)^{2-}$	**6c**	1865.1(m)	1731.0(s)[c]	–	–	1798
$W(CO)_3(S,S\text{-}C_6H_4)^{2-}$	**7c**	1867.9(m)	1745.5(s)[c]	–	–	1807

[a] As the PPN salt. [b] Spectra determined in THF. [c] Spectra determined in CH_3CN.

Table 3. Average ν(CO) Frequency in $M(CO)_3((X,Y\text{-}C_6H_4)^{2-}$ Derivatives

complex	av ν(C≡O), cm^{-1}	ref
$Cr(CO)_3(NH,S\text{-}C_6H_4)^{2-}$	1792	this work[a]
$Cr(CO)_3(dtb\text{-}O,O\text{-}C_6H_4)^{2-}$	1801	10[a]
$Cr(CO)_3(O,S\text{-}C_6H_4)^{2-}$	1805	this work[b]
$Mo(CO)_3(dtb\text{-}O,O\text{-}C_6H_4)^{2-}$	1801	10[a]
$Mo(CO)_3(NH,S\text{-}C_6H_4)^{2-}$	1802	this work[b]
$Mo(CO)_3(O,S\text{-}C_6H_4)^{2-}$	1808	this work[b]
$W(CO)_3(NH,NH\text{-}C_6H_4)^{2-}$	1773	11[a]
$W(CO)_3(NH,O\text{-}C_6H_4)^{2-}$	1783	11[a]
$W(CO)_3(NH,S\text{-}C_6H_4)^{2-}$	1789	this work[b]
$W(CO)_3(dtb\text{-}O,O\text{-}C_6H_4)^{2-}$	1790	10[a]
$W(CO)_3(O,O\text{-}C_6H_4)^{2-}$	1795	9[a]
$W(CO)_3(O,S\text{-}C_6H_4)^{2-}$	1798	this work[b]
$W(CO)_3(S,S\text{-}C_6H_4)^{2-}$	1807	this work[b]

[a] As the tetraethylammonium salt. [b] As the PPN salt.

basis set. Density functional calculations (B3LYP)[16−18] were also performed on a couple of complexes for comparitive purposes. The two geometries were almost identical, therefore the less expensive HF calculations were used for the remainder of the study. Single-shot energy calculations were performed at the HF geometries using density functional theory with the B3LYP functional.

Results

Synthesis, Spectral, and Structural Characterization. $[PPN]_2[M(CO)_3X]$ and $[PPN]_2[M(CO)_4X]$. Several eighteen- and sixteen-electron derivatives of zerovalent group 6 metal carbonyl complexes have been synthesized using a series of 1,2-disubstituted benzene rings with varying oxygen, nitrogen, and sulfur donor atoms. The reactions occur in better than 78% yield by the labile ligand displacement reaction between $M(CO)_5THF$, obtained via photolysis of $Cr(CO)_6$, $Mo(CO)_6$, or $W(CO)_6$ in tetrahydrofuran, with the singly deprotonated PPN salts of 2-aminothiophenol (NH_2,SH-C_6H_4), 2-hydroxythiophenol (OH,SH-C_6H_4), or dithiobenzene (SH,SH-C_6H_4) (complexes **1**−**7**). Scheme 2 uses 2-hydroxythiophenol to summarize the approach employed in the synthesis of complexes **1**−**7**. The

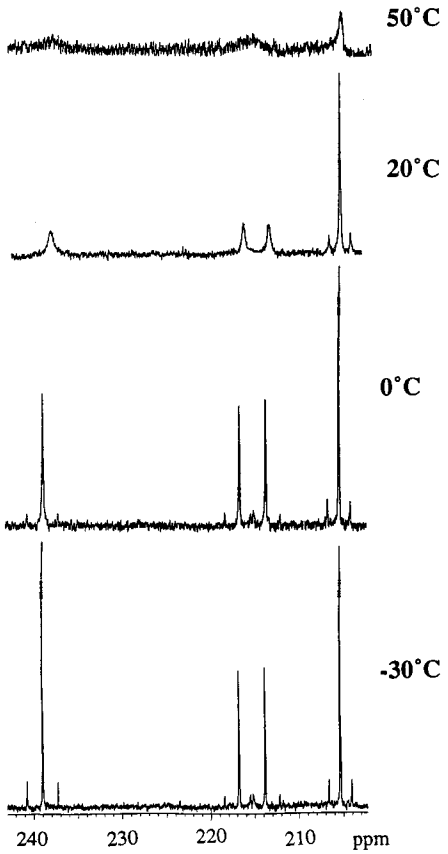

Figure 1. Variable temperature ^{13}C NMR spectra for **5c** + ^{13}CO ⇌ **5b**.

reaction proceeds, as evident by the time-dependent ν(CO) infrared spectrum(see Table 2), by way of the displacement of THF by the deprotonated sulfur atom (**1a**−**7a**). The addition of another equivalent of base is followed shortly by the chelation to the metal center with concomitant loss of CO to produce the metal tetracarbonyl ligand complex exhibiting a four-band pattern in the carbonyl region of the infrared spectrum consistent with a *cis*-disubstituted tetracarbonylmetal center (**1b**−**7b**). Depending on the metal and the ligand, this complex may spontaneously dissociate CO to form the tricarbonyl complex

(16) Becke, A. D. *Phys. Rev. A.* **1988**, *38*, 3098.
(17) Becke, A. D. *J. Chem. Phys.* **1993**, *98*, 5648.
(18) Lee, C.; Yang, W.; Parr, R. G. *Phy. Rev. B* **1988**, *37*, 785.

Table 4. ^{13}C NMR Data for the Carbonyl Ligands in $[M(CO)_{4,3}((X,Y\text{-}C_6H_4)]^{2-}$ Anions[a,b]

complex		^{13}C resonance, ppm		
		CO (axial)	CO (equatorial)	
$Mo(CO)_4(O,S\text{-}C_6H_4)^{2-}$	**3b**	209.2	222.7	227.5
$Mo(CO)_4(NH,S\text{-}C_6H_4)^{2-}$	**4b**	211.4	223.8	227.4
$W(CO)_4(NH,S\text{-}C_6H_4)^2$	**5b**	205.4	213.9	216.9
		$^1J_{W-C} = 120$ Hz	$^1J_{W-C} = 160$ Hz	$^1J_{W-C} = 162$ Hz
$W(CO)_4(O,S\text{-}C_6H_4)^2$	**6b**	206.9	215.8	219.7
		$^1J_{W-C} = 130$ Hz	$^1J_{W-C} = 170$ Hz	$^1J_{W-C} = 156$ Hz
$W(CO)_4(S,S\text{-}C_6H_4)^2$	**7b**	205.1	217.9	
		$^1J_{W-C} = 120$ Hz	$^1J_{W-C} = 160$ Hz	
$Cr(CO)_3(NH,S\text{-}C_6H_4)^{2-}$	**1c**		249.8	
$Cr(CO)_3(O,S\text{-}C_6H_4)^{2-}$	**2c**		247.3	
$Mo(CO)_3(NH,S\text{-}C_6H_4)^{2-}$	**3c**		242.1	
$Mo(CO)_3(O,S\text{-}C_6H_4)^{2-}$	**4c**		240.0	
$W(CO)_3(NH,S\text{-}C_6H_4)^2$	**5c**		239.1	
			$^1J_{W-C} = 176$ Hz	
$W(CO)_3(O,S\text{-}C_6H_4)^2$	**6c**		236.0	
			$^1J_{W-C} = 180$ Hz	
$W(CO)_3(S,S\text{-}C_6H_4)^2$	**7c**		236.2	
			$^1J_{W-C} = 130$ Hz	

[a] Spectra determined in acetonitrile-d_3. [b] PPN salt.

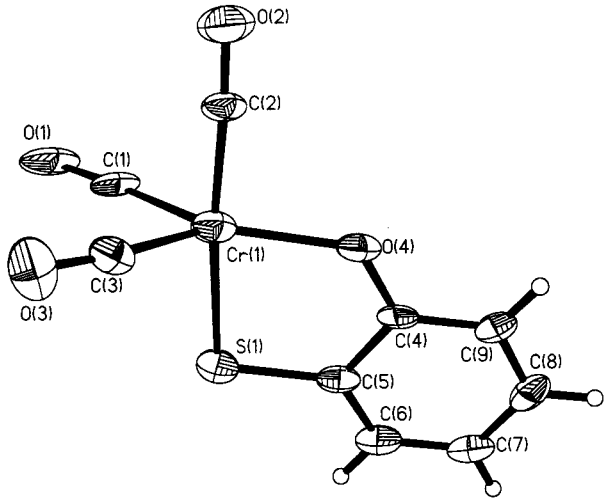

Figure 2. Thermal ellipsoid drawing of the anion of complex **2c** with atomic numbering scheme.

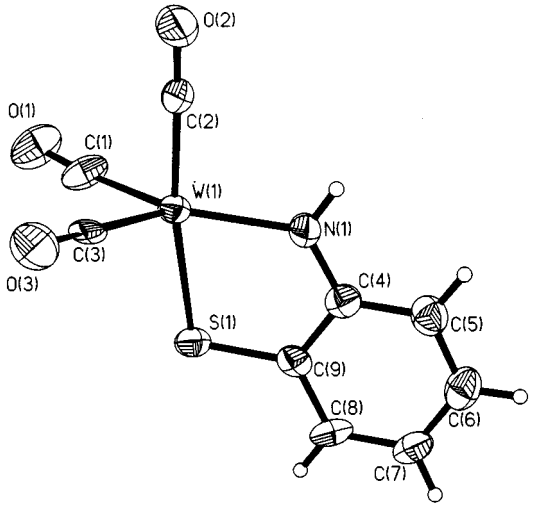

Figure 3. Thermal ellipsoid drawing of the anion of complex **5c** with atomic numbering scheme.

Scheme 3

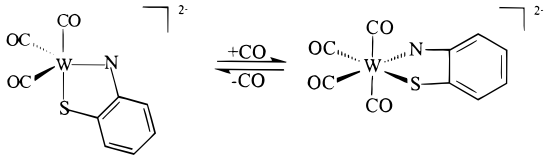

(**1c**−**7c**); however, some metal and ligand combinations require either gentle heating (40 °C) and/or an argon purge to facilitate CO dissociation. The synthesis of the tungsten tetracarbonyl derivative of 1,2-diphosphinobenzene (**8**) has been accomplished in good yield via the labile ligand displacement reaction between $W(CO)_4(piperidine)_2$ and neutral 1,2-diphosphinobenzene.

The infrared frequencies of the pentacarbonyl, tetracarbonyl, and tricarbonyl derivatives of the metal ligand complex are provided in Table 2. The pentacarbonyl derivatives, **1a**−**7a**, display a three-band pattern in the ν(CO) region of the infrared consistent with a monosubstituted pentacarbonyl. Complexes **1b**−**7b** exhibit a four-band pattern in the carbonyl region typical of a *cis*-disubstituted tetracarbonyl. The tricarbonyl derivatives, **1c**−**7c**, demonstrate a two-band pattern consisting of a medium sharp peak and a large broad peak, consistent with a tricarbonyl derivative of approximately C_{3v} symmetry. CO ligands are good probes of the electron-donating ability of the ancillary ligands in metal carbonyl derivatives. It is of interest to compare the average ν(CO) values of each tricarbonyl derivative reported upon herein with each other and with other tricarbonyl species of this nature.[9−11] That is, in $[M(CO)_3X]^{2-}$, the average ν(CO) values should shift to lower frequencies as X becomes a better π-donor. The average ν(CO) frequencies for a number of low valent group 6 tricarbonyl derivatives, including Cr(0), Mo(0) and W(0) tricarbonyl derivatives of 3,5-di-*tert*-butylcatecholate-(dtb-O,O-$C_6H_4)^{2-}$, 2-amidophenoxide, and diamidobenzene,[9−11] are provided in Table 3.

Table 4 lists the ^{13}C NMR data for complexes **3b**−**7b** and **1c**−**7c** in the CO regions of the spectra. Chemical shift data for the metal tetracarbonyl moieties reveal a slight electronic difference between the CO ligand trans to oxygen versus the CO ligand trans to nitrogen. The ^{13}C NMR spectra of complexes **3b**−**6b** display three signals for the carbonyl carbons in an approximate 2:1:1 intensity ratio. The more intense resonance for the two carbonyl ligands cis to both π-donors is observed upfield from the two smaller signals assigned to the carbonyl ligands trans to one π-donor. On the other hand, the ^{13}C NMR spectrum of the symmetrically substituted derivative, **7b**, reveals

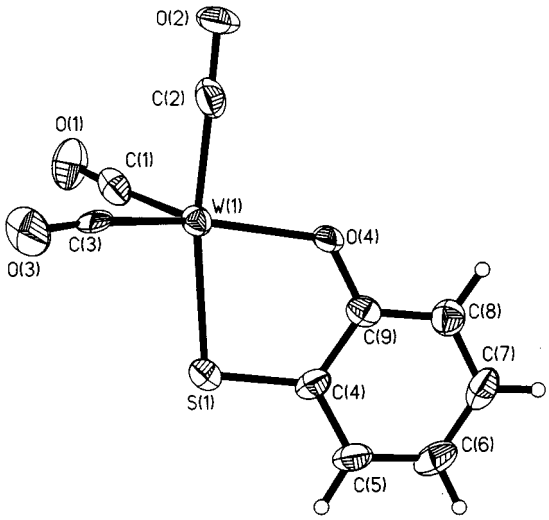

Figure 4. Thermal ellipsoid drawing of the anion of complex **6c** with atomic numbering scheme.

Table 5. Bond Lengths [Å] and Angles [deg] for the Dianion, $[Cr(CO)_3(O,S\text{-}C_6H_4)]^{2-}$, of **2c**[a]

Cr(1)−C(1)	1.793(10)	O(3)−C(3)	1.207(10)
Cr(1)−C(2)	1.814(9)	O(4)−C(4)	1.333(10)
Cr(1)−C(3)	1.758(10)	C(4)−C(9)	1.390(12)
Cr(1)−O(4)	1.986(6)	C(4)−C(5)	1.432(12)
Cr(1)−S(1)	2.372(3)	C(5)−C(6)	1.371(12)
S(1)−C(5)	1.749(9)	C(6)−C(7)	1.392(13)
O(1)−C(1)	1.186(10)	C(7)−C(8)	1.416(12)
O(2)−C(2)	1.186(10)	C(8)−C(9)	1.372(12)
O(1)−C(1)−Cr(1)	175.7(8)	C(3)−Cr(1)−C(1)	81.1(4)
O(2)−C(2)−Cr(1)	176.5(8)	C(3)−Cr(1)−C(2)	85.6(4)
O(3)−C(3)−Cr(1)	175.1(8)	C(1)−Cr(1)−C(2)	92.3(4)
O(4)−C(4)−C(9)	121.9(8)	C(3)−Cr(1)−O(4)	133.4(3)
O(4)−C(4)−C(5)	119.3(8)	C(1)−Cr(1)−O(4)	145.5(4)
C(9)−C(4)−C(5)	118.9(8)	C(2)−Cr(1)−O(4)	91.8(3)
C(6)−C(5)−C(4)	118.3(9)	C(3)−Cr(1)−S(1)	100.3(3)
C(6)−C(5)−S(1)	124.9(7)	C(1)−Cr(1)−S(1)	90.4(3)
C(4)−C(5)−S(1)	116.8(7)	C(2)−Cr(1)−S(1)	173.9(3)
C(5)−C(6)−C(7)	123.6(9)	O(4)−Cr(1)−S(1)	82.9(2)
C(6)−C(7)−C(8)	116.8(9)	C(5)−S(1)−Cr(1)	98.0(3)
C(9)−C(8)−C(7)	121.1(9)	C(4)−O(4)−Cr(1)	122.8(5)
C(8)−C(9)−C(4)	121.1(9)		

[a] Estimated standard deviations are given in parentheses.

two CO ^{13}C NMR signals in a 1:1 intensity ratio. The resonance for the two carbonyl ligands cis to both sulfurs is upfield of the signal due to the carbonyls trans to sulfur. Each resonance for complexes **5b**−**7b** reveals satellites due to coupling with the ^{183}W nucleus. Appropriate coupling constants are listed in Table 4.

The ^{13}C NMR spectra of complexes **1c**−**7c** in acetonitrile (concentrated ∼0.05 M) in the presence of one atmosphere of ^{13}CO (solubility $\sim 6 \times 10^{-3}$ M) display resonances in the carbonyl region due to both tri- and tetracarbonyl dianions. Figure 1 depicts a representative assembly of temperature-dependent ^{13}C NMR spectra for the mixture of complexes $[PPN]_2[W(CO)_4(NH,S\text{-}C_6H_4)]$ (**5b**) and $[PPN]_2[W(CO)_3(NH,S\text{-}C_6H_4)]$ (**5c**). In all complexes studied the ^{13}C signals are broad near ambient temperature or above. This is the result of a rapid *intermolecular* exchange process between the tri- and tetracarbonyl species as illustrated for complexes **5b** and **5c** in Scheme 3. The ratio of tricarbonyl to tetracarbonyl dianions was found to decrease in going from chromium to tungsten, where under this set of conditions the chromium form is mostly tricarbonyl and the tungsten species is mostly tetracarbonyl. However, in all cases the equilibrium constant for the process defined in

Table 6. Bond Lengths [Å] and Angles [deg] for the Dianion, $[W(CO)_3(NH,S\text{-}C_6H_4)]^{2-}$, of **5c**[a]

W(1)−C(3)	1.902(8)	O(3)−C(3)	1.182(10)
W(1)−C(1)	1.913(9)	N(1)−C(4)	1.364(11)
W(1)−C(2)	1.942(9)	C(4)−C(5)	1.407(13)
W(1)−N(1)	2.106(7)	C(4)−C(9)	1.415(12)
W(1)−S(1)	2.501(2)	C(5)−C(6)	1.380(13)
S(1)−C(9)	1.732(9)	C(6)−C(7)	1.400(14)
O(1)−C(1)	1.196(11)	C(7)−C(8)	1.389(13)
O(2)−C(2)	1.165(11)	C(8)−C(9)	1.411(12)
C(3)−W(1)−C(1)	85.4(4)	O(2)−C(2)−W(1)	176.0(9)
C(3)−W(1)−C(2)	83.3(4)	O(3)−C(3)−W(1)	174.9(7)
C(1)−W(1)−C(2)	88.2(4)	N(1)−C(4)−C(5)	123.3(8)
C(3)−W(1)−N(1)	126.1(3)	N(1)−C(4)−C(9)	117.4(8)
C(1)−W(1)−N(1)	148.5(4)	C(5)−C(4)−C(9)	119.3(8)
C(2)−W(1)−N(1)	94.8(3)	C(6)−C(5)−C(4)	120.9(9)
C(3)−W(1)−S(1)	103.1(2)	C(5)−C(6)−C(7)	121.0(9)
C(1)−W(1)−S(1)	98.0(3)	C(8)−C(7)−C(6)	118.3(8)
C(2)−W(1)−S(1)	171.4(3)	C(7)−C(8)−C(9)	122.4(9)
N(1)−W(1)−S(1)	76.9(2)	C(8)−C(9)−C(4)	118.2(8)
C(9)−S(1)−W(1)	100.5(3)	C(8)−C(9)−S(1)	123.4(7)
C(4)−N(1)−W(1)	126.0(6)	C(4)−C(9)−S(1)	118.3(6)
O(1)−C(1)−W(1)	175.4(9)		

[a] Estimated standard deviations are given in parentheses.

Table 7. Bond Lengths [Å] and Angles [deg] for the Dianion, $[W(CO)_3(O,S\text{-}C_6H_4)]^{2-}$, of **6c**[a]

W(1)−C(3)	1.887(12)	O(3)−C(3)	1.217(13)
W(1)−C(1)	1.910(13)	O(4)−C(9)	1.321(11)
W(1)−C(2)	1.923(11)	C(4)−C(5)	1.392(13)
W(1)−O(4)	2.085(6)	C(4)−C(9)	1.423(13)
W(1)−S(1)	2.482(3)	C(5)−C(6)	1.382(14)
S(1)−C(4)	1.727(10)	C(6)−C(7)	1.37(2)
O(2)−C(2)	1.204(12)	C(7)−C(8)	1.357(14)
O(1)−C(1)	1.188(12)	C(8)−C(9)	1.390(13)
C(3)−W(1)−C(1)	80.9(5)	C(6)−C(5)−C(4)	121.1(10)
C(3)−W(1)−C(2)	91.4(4)	C(7)−C(6)−C(5)	120.7(10)
C(1)−W(1)−C(2)	82.9(4)	C(8)−C(7)−C(6)	119.1(10)
C(3)−W(1)−O(4)	144.7(4)	C(7)−C(8)−C(9)	122.6(10)
C(1)−W(1)−O(4)	134.3(3)	O(4)−C(9)−C(8)	122.1(9)
C(2)−W(1)−O(4)	91.7(3)	O(4)−C(9)−C(4)	119.5(8)
C(3)−W(1)−S(1)	96.4(3)	C(8)−C(9)−C(4)	118.5(9)
C(1)−W(1)−S(1)	104.0(3)	O(1)−C(1)−W(1)	176.5(9)
C(2)−W(1)−S(1)	170.3(3)	O(3)−C(3)−W(1)	171.9(9)
O(4)−W(1)−S(1)	78.6(2)	C(5)−C(4)−C(9)	118.0(9)
C(4)−S(1)−W(1)	99.2(3)	C(5)−C(4)−S(1)	123.9(8)
C(9)−O(4)−W(1)	124.6(6)	C(9)−C(4)−S(1)	118.1(7)
O(2)−C(2)−W(1)	176.9(9)		

[a] Estimated standard deviations are given in parentheses.

Scheme 3 specifically for **5c** + CO ⇌ **5b** is greater than zero. That is, the tetracarbonyl species are thermodynamically favored over the tricarbonyl complexes plus carbon monoxide. Within a metal series the equilibrium position is a function of the π-donating ability of the appended ligands, e.g., the concentration ratio of $W(CO)_3(NH,S\text{-}C_6H_4)^{2-}/W(CO)_4(NH,S\text{-}C_6H_4)^{2-}$ (**5b**/**5c**) is greater than that of $W(CO)_3(O,S\text{-}C_6H_4)^{2-}/W(CO)_4(O,S\text{-}C_6H_4)^{2-}$ (**6c**/**6b**) at the same [CO]. As anticipated, the stronger π-donating amido ligand stabilizes the "16-electron" species to a greater extent than the phenoxide ligand. In other words at a given temperature equilibrium process **5c** + CO ⇌ **5b** lies further to the left than that of **6c** + CO ⇌ **6b**. In addition it is clear that the three inequivalent carbonyl ligands in the tricarbonyl dianions are fluxional at the lowest temperature attained(−30 to −40 °C), as previously observed in other closely related derivatives.[9−11] This is indicative of a low-energy barrier for *intramolecular* CO exchange, as is generally noted in five-coordinate metal carbonyl derivatives.

The structures of complexes **2c**, **5c**, and **6c** have been determined by crystallographic analysis; thermal ellipsoid

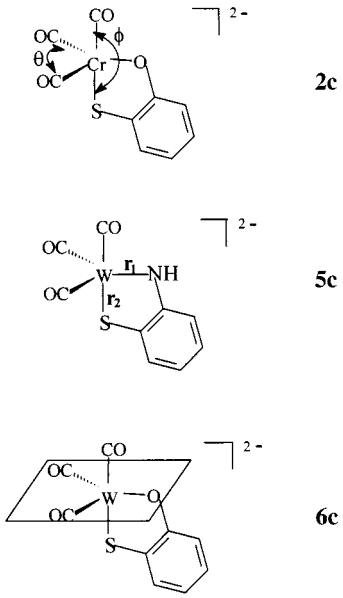

Figure 5. Schematic drawings of complexes **2c**, **5c**, and **6c** where the dianions are represented ideally as having trigonal bipyramidal geometry.

Table 8. Comparative Structural Parameters for Tungsten Tricarbonyl Dianions

complex	r_1 (Å)	r_2 (Å)	θ (deg)	ϕ (deg)	dev. from planarity (Å)
$W(CO)_3(NH,NH\text{-}C_6H_4)^{2-}$	2.125	2.156	82.2	166.4	0.003
$W(CO)_3(NH,O\text{-}C_6H_4)^{2-}$	2.078	2.143	83.3	170.7	0.005
$W(CO)_3$(dtb-O,O-$C_6H_4)^{2-}$ [a]	2.059	2.154	85.6	166.7	0.026
$W(CO)_3(NH,S\text{-}C_6H_4)^{2-}$	2.105	2.501	85.3	171.4	0.0184
$W(CO)_3(O,S\text{-}C_6H_4)^{2-}$	2.085	2.482	80.9	170.3	0.0214
$Mo(CO)_3$(dtb-O,O-$C_6H_4)^{2-}$ [a]	2.083	2.193	85.5	168.5	0.0773
$Cr(CO)_3$(dtb-O,O-$C_6H_4)^{2-}$ [a]	1.924	2.048	80.0	146.8	0.0419
$Cr(CO)_3(O,S\text{-}C_6H_4)^{2-}$	1.986	2.372	81.1	173.9	0.0150

[a] dtb-O,O-$C_6H_4^{2-}$ = 3,5-di-*tert*-butylcatecholate.

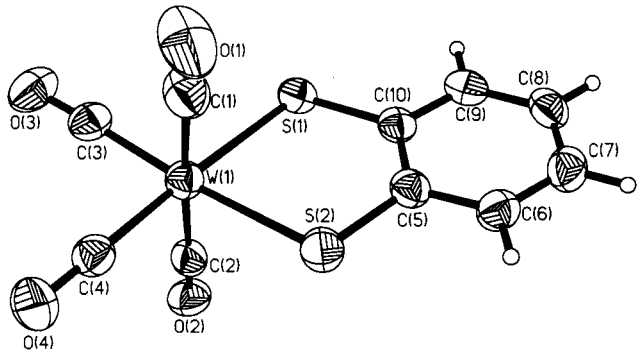

Figure 6. Thermal ellipsoid drawing of the anion of complex **7b** with atomic numbering scheme.

drawings of the dianions are provided in Figures 2−4 with selected bond lengths and angles in Tables 5−7. The dianions of complexes **2c, 5c**, and **6c** consist of a 2-hydroxythiophenolate (**2c**, **6c**) or a 2-amidothiophenolate (**5c**) residue that forms a five-membered chelate ring to the $M(CO)_3$ center through its deprotonated thiol and hydroxyl (**2c**, **6c**) or amino (**5c**) groups. Two PPN cations are present to balance the charge. Noninteracting solvent molecules were found in the crystal lattices of all three compounds, i.e., **2c** (CH_3CN and CH_3OH), **5c** ($4CH_3CN$), **6c** ($2CH_3CN$). The geometry of the five-coordinate metal center is that of a distorted trigonal bipyramid. The equatorial

Table 9. Bond Lengths [Å] and Angles [deg] for the Dianion, $[W(CO)_4(S,S\text{-}C_6H_4)]^{2-}$, of **7b**[a]

W(1)−C(3)	1.944(5)	O(2)−C(2)	1.159(5)
W(1)−C(4)	1.947(5)	O(3)−C(3)	1.175(5)
W(1)−C(2)	2.015(5)	O(4)−C(4)	1.174(5)
W(1)−C(1)	2.045(5)	C(5)−C(6)	1.399(6)
W(1)−S(2)	2.5451(11)	C(5)−C(10)	1.410(6)
W(1)−S(1)	2.5520(11)	C(6)−C(7)	1.387(6)
S(1)−C(10)	1.763(4)	C(7)−C(8)	1.381(7)
S(2)−C(5)	1.755(4)	C(8)−C(9)	1.383(6)
O(1)−C(1)	1.141(6)	C(9)−C(10)	1.401(6)
C(3)−W(1)−C(4)	86.6(2)	C(3)−W(1)−S(1)	95.56(14)
C(3)−W(1)−C(2)	89.9(2)	C(4)−W(1)−S(1)	176.96(13)
C(4)−W(1)−C(2)	89.9(2)	C(2)−W(1)−S(1)	87.97(12)
C(3)−W(1)−C(1)	93.2(2)	C(1)−W(1)−S(1)	90.81(14)
C(4)−W(1)−C(1)	91.2(2)	S(2)−W(1)−S(1)	81.23(3)
C(2)−W(1)−C(1)	176.8(2)	C(10)−S(1)−W(1)	106.32(14)
C(3)−W(1)−S(2)	175.53(13)	C(5)−S(2)−W(1)	106.43(14)
C(4)−W(1)−S(2)	96.76(13)	O(1)−C(1)−W(1)	176.7(5)
C(2)−W(1)−S(2)	93.06(12)	O(3)−C(3)−W(1)	177.2(4)
C(1)−W(1)−S(2)	83.8(2)	O(4)−C(4)−W(1)	177.5(4)
O(2)−C(2)−W(1)	177.7(4)	C(5)−C(10)−S(1)	122.6(3)
C(6)−C(5)−C(10)	118.7(4)	C(9)−C(10)−C(5)	118.4(4)
C(6)−C(5)−S(2)	118.2(3)	C(9)−C(10)−S(1)	119.0(3)
C(10)−C(5)−S(2)	123.1(3)	C(6)−C(7)−C(8)	120.1(4)
C(7)−C(6)−C(5)	121.5(4)	C(9)−C(8)−C(7)	119.0(4)
C(8)−C(9)−C(10)	122.3(4)		

[a] Estimated standard deviations are given in parentheses.

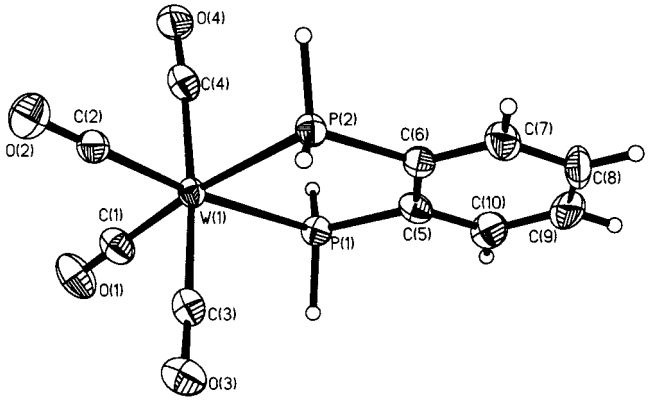

Figure 7. Thermal ellipsoid drawing of the anion of complex **8** with atomic numbering scheme.

plane consists of two carbonyl ligands, the metal center and one of the π-donating atoms of the chelating ligand. The axial positions contain the remaining carbonyl ligand and π-donating atom. In each case, the stronger π-donor is located in the equatorial position. In the chromium derivative, the average Cr-CO bond distance is 1.788(10) Å and the Cr−S bond distance is 2.372(3) Å. The oxygen donor atom is located in the equatorial plane; the Cr−O bond distance is 1.986(6) Å. The bite angle of the chelate ring is 82.9(2)° in **2c**.

The average W-CO bond length in **5c**, $W(CO)_3(NH,S\text{-}C_6H_4)^{2-}$, is 1.919(9) Å, somewhat longer than the average W-CO bond distance of 1.907(12) Å found in $W(CO)_3(O,S\text{-}C_6H_4)^{2-}$ (**6c**). In $W(CO)_3(NH,S\text{-}C_6H_4)^{2-}$ (**5c**), the nitrogen is located in the equatorial plane. The W−N bond distance is 2.106(7) Å while the W−S bond length is 2.501(2) Å. In the $W(CO)_3(O,S\text{-}C_6H_4)^{2-}$ derivative (**6c**), the W−O bond distance is 2.085(6) Å and the W−S bond length is 2.482(3) Å, somewhat shorter than the W−S bond in the $W(CO)_3(NH,S\text{−}Ph)^{2-}$ derivative. The shortening of the axial ligand in **6c** vs **5c** is due to the weaker π-donation of oxygen relative to nitrogen. This results in a greater electron deficiency at the tungsten center and hence an increase in π-donation from the sulfur and a

Table 10. Bond Lengths [Å] and Angles [deg] for $W(CO)_4(PH_2,PH_2\text{-}C_6H_4)$, **8**[a]

W(1)−C(2)	1.992(11)	O(2)−C(2)	1.165(13)
W(1)−C(1)	2.005(12)	O(3)−C(3)	1.149(13)
W(1)−C(3)	2.014(10)	O(4)−C(4)	1.156(14)
W(1)−C(4)	2.034(11)	C(5)−C(10)	1.41(2)
W(1)−P(1)	2.465(3)	C(5)−C(6)	1.402(14)
W(1)−P(2)	2.466(2)	C(6)−C(7)	1.392(14)
P(1)−C(5)	1.818(10)	C(7)−C(8)	1.37(2)
P(2)−C(6)	1.840(10)	C(8)−C(9)	1.36(2)
O(1)−C(1)	1.153(14)	C(9)−C(10)	1.40(2)
C(2)−W(1)−C(1)	96.4(4)	C(6)−P(2)−W(1)	111.7(3)
C(2)−W(1)−C(3)	87.7(4)	O(1)−C(1)−W(1)	177.6(10)
C(1)−W(1)−C(3)	88.3(4)	O(2)−C(2)−W(1)	178.9(9)
C(2)−W(1)−C(4)	86.2(4)	O(3)−C(3)−W(1)	177.8(9)
C(1)−W(1)−C(4)	91.8(4)	O(4)−C(4)−W(1)	175.3(10)
C(3)−W(1)−C(4)	173.9(4)	C(10)−C(5)−C(6)	119.0(10)
C(2)−W(1)−P(1)	170.7(3)	C(10)−C(5)−P(1)	122.2(8)
C(1)−W(1)−P(1)	92.9(3)	C(6)−C(5)−P(1)	118.7(8)
C(3)−W(1)−P(1)	94.0(3)	C(7)−C(6)−C(5)	119.7(10)
C(4)−W(1)−P(1)	92.1(3)	C(7)−C(6)−P(2)	122.4(8)
C(2)−W(1)−P(2)	91.8(3)	C(5)−C(6)−P(2)	117.9(7)
C(1)−W(1)−P(2)	171.8(3)	C(8)−C(7)−C(6)	121.0(11)
C(3)−W(1)−P(2)	91.1(3)	C(9)−C(8)−C(7)	119.9(11)
C(4)−W(1)−P(2)	89.6(3)	C(8)−C(9)−C(10)	121.6(11)
P(1)−W(1)−P(2)	79.03(8)	C(5)−C(10)−C(9)	118.8(11)
C(5)−P(1)−W(1)	112.0(3)		

[a] Estimated standard deviations are given in parentheses.

Table 11. Comparison of Selected Experimental and Calculated Bond Lengths [Å] and Angles [deg] in $[W(CO)_3(NH,S\text{-}C_6H_4)]^{2-}$, **5c**

	HF	B3LYP	Experimental
W−S	2.649	2.630	2.501(2)
W−N	2.122	2.110	2.106(7)
$W-C_{ax}$	1.937	1.936	1.942(9)
$W-C_{eq}$	1.953	1.939	1.902(8), 1.913(9)
$C_{eq}-W-C_{eq}$	86.2	86.9	85.4(4)
$C_{eq}-W-C_{ax}$	90.5	90.3	83.3(8), 88.2(4)
N−W−S	76.0	76.5	76.9(2)
$C_{eq}-W-S$	136.8	136.5	126.1(3), 148.5(4)
$C_{ax}-W-S$	168.5	168.7	171.4(3)

Table 12. Comparison of Calculated Bond Lengths [Å] and Angles [deg] in $[W(CO)_4(NH,S\text{-}C_6H_4)]^{2-}$, **5b**

	HF	B3LYP
W−S	2.698	2.677
W−N	2.215	2.183
$W-C_{trans-S}$	1.949	1.951
$W-C_{trans-N}$	1.971	1.976
$W-C_{cis-S,N}$	2.055	2.029
$C_{trans-S}-W-C_{trans-N}$	91.2	92.3
$C_{cis}-W-C_{cis}$	178.4	172.9
N−W−S	75.4	76.2
$S-W-C_{trans-S}$	172.1	171.4
$S-W-C_{trans-N}$	96.7	96.2
$N-W-C_{trans-N}$	172.1	172.5
$N-W-C_{trans-S}$	96.7	95.2

therefore a shorter W−S distance. Finally, the bite angle of the chelate ring is similar in both the $W(CO)_3(O,S\text{-}C_6H_4)^{2-}$ derivative (78.6(2)°) and in the $W(CO)_3(NH,S\text{-}C_6H_4)^{2-}$ complex (76.9(2)°). In each case, the sulfur donor atom is located in the axial position, indicating that the O- and N-donor atoms, respectively, are the better π-donors.

Figure 5 provides schematic drawings of **2c**, **5c**, and **6c** where their geometry is represented as trigonal bipyramidal. However, the structural parameters indicated in Figure 5 and summarized in Table 8 reveal that significant distortions from trigonal bipyramidal are observed. Also included, for purposes of comparison, are those parameters for the 16-electron, tricarbonyl

Table 13. Ab Initio Calculations of W and Cr 16- and 18-Electron Complexes (kJ/mol)

complex	HF	B3LYP single-shot[b]
$[W(CO)_4(NH,NH\text{-}C_6H_4)]^{2-}$	0.000	0.000
$[W(CO)_3(NH,NH\text{-}C_6H_4)]^{2-}$	21.724	82.109
$[W(CO)_4(NH,O\text{-}C_6H_4)]^{2-}$	0.000	0.000
$[W(CO)_3(NH,O\text{-}C_6H_4)]^{2-}$	38.899	97.153
$[W(CO)_4(NH,S\text{-}C_6H_4)]^{2-}$	0.000	0.000
$[W(CO)_3(NH,S\text{-}C_6H_4)]^{2-}$	49.704	103.865
$[W(CO)_4(O,O\text{-}C_6H_4)]^{2-}$	0.000	0.000
$[W(CO)_3(O,O\text{-}C_6H_4)]^{2-}$	60.898	119.646
$[W(CO)_4(O,S\text{-}C_6H_4)]^{2-}$	0.000	0.000
$[W(CO)_3(O,S\text{-}C_6H_4)]^{2-}$	68.546	122.968
$[W(CO)_3(S,O\text{-}C_6H_4)]^{2-}$	78.968	127.262
$[W(CO)_4(S,S\text{-}C_6H_4)]^{2-}$	0.000	0.000
$[W(CO)_3(S,S\text{-}C_6H_4)]^{2-}$	85.871	132.445
$[Cr(CO)_4(O,O\text{-}C_6H_4)]^{2-}$	0.000	−
$[Cr(CO)_3(O,O\text{-}C_6H_4)]^{2-}$	45.671	−
$[Cr(CO)_4(O,S\text{-}C_6H_4)]^{2-}$	0.000	−
$[Cr(CO)_3(O,S\text{-}C_6H_4)]^{2-}$	54.045	−

[a] Energies relative to the 18-electron complex in each set. [b] Single-shot energy calculations done at the HF geometry.

Table 14. Comparison of Selected Experimental (in Parentheses) and Calculated Bond Lengths [Å] and Angles [deg] in **1**, $[W(CO)_3(O,S\text{-}C_6H_4)]^{2-}$ (**6c**), and $[W(CO)_3(S,O\text{-}C_6H_4)]^{2-}$ (**6d**)

	$[W(CO)_3(O,S\text{-}C_6H_4)]^{2-}$ [a]	$[W(CO)_3(S,O\text{-}C_6H_4)]^{2-}$ [b]
W−S	2.664 (2.482(3))	2.622
W−O	2.110 (2.085(6))	2.160
$W-C_{eq}$	1.942 (1.899[12])	1.937
$W-C_{ax}$	1.945 (1.923(11))	1.949
O−W−S	75.5 (78.6(2))	75.6
$C_{eq}-W-C_{eq}$	85.4 (80.9(5))	86.8
$C_{eq}-W-C_{ax}$	90.5 (87.2[4])	90.1
$X_{eq}-W-C_{eq}$	137.2 (139.5[4])	136.5
$X_{eq}-W-C_{ax}$	91.6 (91.7(3))	98.2
$X_{ax}-W-C_{ax}$	167.1 (170.3(3))	168.5
$X_{ax}-W-C_{eq}$	98.9 (100.2(3))	98.2

[a] S in the axial position O in the equatorial position. [b] S in the equatorial position O in the axial position.

complexes published in studies prior to this one, including the W, Mo, or Cr tricarbonyl derivatives of 3,5-di-*tert*-butylcatecholate, 2-amidophenoxide, and diamidobenzene.[9−11]

Bright red crystals of the tungsten tetracarbonyl derivative of dithiobenzene, complex **7b**, were obtained by the slow diffusion of diethyl ether into a concentrated CH_3CN solution of the complex. Figure 6 shows a drawing of the dianion while selected bond angles and lengths are listed in Table 9. The structure of $W(CO)_4(S,S\text{-}C_6H_4)^{2-}$ consists of a tungsten tetracarbonylmetal center chelated by doubly deprotonated dithiophenolate; the charge is balanced by the presence of two PPN cations. The geometry of the metal center is that of a distorted octahedron; the average W-C bond length of the carbonyls trans to sulfur is 1.946(5) Å, and the average bond length of the carbonyls cis to the sulfurs is 1.930(5) Å. The W−S bond lengths are 2.552(1) and 2.545(1) Å, significantly longer than the W−S bond lengths observed in the $W(CO)_3(O,S\text{-}C_6H_4)^{2-}$ (2.482(3) Å) and $W(CO)_3(NH,S\text{-}C_6H_4)^{2-}$ (2.501(2) Å) unsaturated derivatives.

Yellow-brown X-ray-quality crystals were obtained for complex **8**, $W(CO)_4(PH_2,PH_2\text{-}C_6H_4)$, via sublimation at 40 °C. The instability of the doubly deprotonated analogue of **8** prevented examination of the π-donor character of the phosphido group. A thermal ellipsoid drawing of complex **8** is given in Figure 7; bond lengths and angles are listed in Table 10. The geometry of the metal center is that of a distorted octahedron.

The structure consists of the diphosphinobenzene ligand bound to a $W(CO)_4$ center with a chelate bite angle of 79.03(8)°. The W-CO bond distances for the carbonyls trans to phosphorus are 2.01(1) and 2.03(1) Å; the average bond length of the two axial CO's, cis to phosphorus, is 2.02(1) Å.

Theoretical Calculations

Ab initio geometry optimizations and energy calculations were performed on a series of related 16e and 18e complexes reported herein. This study was undertaken in order to determine the relative stability of the 16e vs 18e complexes. We have also undertaken an investigation into the bonding between the π-donor and the metal in these systems to determine why the better π-donor occupies an equatorial site in the trigonal bipyramidal geometry of the 16-electron tricarbonyl complexes.

Hartree−Fock geometry optimizations were performed on all complexes, with optimizations using density functional theory being performed on selected complexes for comparative purposes. Both HF and DFT geometry optimizations gave virtually identical results in good agreement with experimentally determined distances and angles, Tables 11 and 12. This is in accord with our previous work which demonstrated that HF and DFT geometry optimizations in tungsten carbonyl anions are very similar.[19] The computationally less expensive HF geometry optimizations were used for the remainder of the computations reported upon here.

The energy differences between the 16- and 18-electron complexes were examined as a measure of the relative stability of the two complexes. In all cases examined, the 18-electron dianion was calculated to be the more stable species. The extent to which the 18-electron complex was more stable was variable depending on which π-donor groups were in the chelating ligand, i.e., the relative stability between the 16- and 18-electron complexes is readily tuned. This energy gap gets increasing large as one goes from good π-donor atoms such as N and O to weaker π-donors such as S, Table 13, the trend in the energy difference between the sixteen- and eighteen-electron complexes is as follows: NH,NH < NH,O < O,O < NH,S < O,S < S,S. This is in conformity with the experimental observations(vide supra) that heat and/or an argon flow are required to form the sixteen electron tricarbonyl complexes in compounds that contain weaker π-donor atoms.

The $[W(CO)_4(O,S\text{-}C_6H_4)]^{2-}/[W(CO)_3(O,S\text{-}C_6H_4)]^{2-}$ system was examined in detail in order to determine why the best π-donor (O in this case) falls in the equatorial position in the 16-electron dianion. Specifically, geometry optimizations were performed on $[W(CO)_4(O,S\text{-}C_6H_4)]^{2-}$ (**6b**) and on the two tricarbonyl isomers of the $[W(CO)_3(O,S\text{-}C_6H_4)]^{2-}$ (**6c**) and $[W(CO)_3(S,O\text{-}C_6H_4)]^{2-}$ (**6d**). From the calculations it was determined that the isomer in which the oxygen atom is in the equatorial plane (**6c**) is about 10.4 kJ/mol more stable than the isomer which contains the sulfur in the equatorial plane (**6d**). This is in agreement with the crystal structure obtained for the tricarbonyl complex, Figure 4, in which the oxygen is indeed in the equatorial plane. Frequency calculations were performed on these three complexes (**6b, 6c, 6d**). From these calculations is was determined that complexes **6b** and **6c** are indeed minima (no negative frequencies) and that complex **6d** is in fact a transition state (one negative frequency). Thermal and zero point corrections on complexes **6b**−**d** lowered the energy about 7−10 kJ/mol, and narrowed the gap between **6b** and **6c** from 68.5 to 61.0 kJ/mol. The gap between the two isomers **6c** and **6d** was also narrowed from 10.4 to 7.7 kJ/mol. These corrections are however not large enough to overcome the energy difference between the sixteen and eighteen complexes, in which the smallest energy gap is 21.7 kJ/mol.

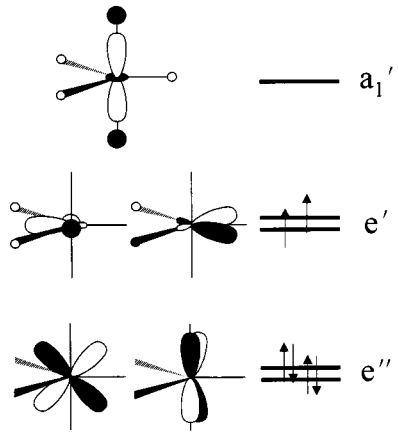

Figure 8. Orbital diagram for the metal d orbitals for idealized trigonal bipyramidal geometry.

The exchange of the axial oxygen and the equatorially positioned sulfur had some effects on the calculated bond distances in the two isomers **6c** and **6d**. The tungsten sulfur bond length was shortened by about 0.04 Å in going from the equatorial position to the axial position, and the tungsten oxygen distance increases 0.05 Å in going from the axial to the equatorial position. Table 14 contains selected bond distances and angles for complexes **6c** and **6d**. This change indicates a stronger ability for the equatorial site to bind a π-donor ligand.

A comparison of the computer generated orbitals in complexes **6c** and **6d** revealed that the orbital structure is very similar, as one might expect. However, there were some subtle differences, most notably was the lower energy of the tungsten-equatorial π-bonding orbitals in complex **6c** versus **6d**. This can be explained based on a general molecular orbital diagram starting from the idealized trigonal bipyramidal geometry shown in Figure 8. The complexes examined here are distorted from idealized trigonal bipyramidal geometry in the following ways. The $C_{eq}-W-C_{eq}$ angle has been reduced to approximately 85°, and the two $C_{eq}-W-X_{eq}$ angles are inequivalent at approximately 125° and 148°. These changes affect the molecular orbital diagram by lowering the energy of the $d_{x^2-y^2}$ orbital with respect to the d_{xy} orbital. The d_{z^2} orbital is also lowered due to deviation from linearity of the $C_{ax}-W-X_{ax}$ angle, however, this orbital is still much higher in energy than the d_{xy} orbital and is therefore not of interest here. The result of these changes is that in a d^6 metal complex only the d_{zy}, d_{yz}, and $d_{x^2-y^2}$ are occupied. The d_{xy} orbital is available for π-donation from the π-donor ligand in the equatorial plane. The stronger the π-donor ligand the more stabilized the d_{xy} orbital will be and the more stable the complex. However, when a π-donor ligand is in the axial position we obtain a situation which Caulton has described as a filled/filled interaction.[20]

Conclusions

Herein the synthesis and characterization of a number of low-valent, group six metal carbonyl complexes containing ancillary ligands capable of π-donation has been described. As expected, the stability of the coordinatively unsaturated, 16-electron complex increases as the ancillary ligand becomes a better

(19) Darensbourg, D. J.; Frost, B. J.; Derecskei-Kovacs, A.; Reibenspies, J. H. *Inorg. Chem.* **1999**, *38*, 4715.

(20) Caulton, K. G. *New J. Chem.* **1994**, *18*, 25.

π-donor. The tungsten tricarbonyl species of 2-amidothiophenolate and 2-hydroxythiophenolate were observed to be relatively stable. Both the 18-electron tetracarbonyl and the 16-electron tricarbonyl derivatives were characterized not only by ν(CO) IR and ^{13}C NMR spectroscopies but also by X-ray crystallography when possible. The structures of these coordinatively unsaturated metal complexes contain a metal tricarbonyl center chelated by the doubly deprotonated ligand under consideration in approximately trigonal bipyramidal geometry. In each case the stronger π-donor atom of the two chelating linkages was observed to prefer the equatorial rather than axial position in trigonal bipyramidal geometry. It was concluded that this phenomenon is due to the availability of an empty orbital of appropriate symmetry in the equatorial plane.

Calculations on these systems have been shown to be in good agreement with the experimentally determined data. It has been demonstrated via ab initio calculations that the tricarbonyl complexes in which the better π-donor is in the equatorial plane are more stable than the same complex with the better π-donor in the axial position. We have also shown that the order of π-donation computed follows that determined from experiment and in is indeed: NH,NH < NH,O < O,O < NH,S < O,S < S,S. This was determined computationally by comparing the energy differences between the sixteen and eighteen electron complex of each ligand and ordering them based on the smallest energy gap equals the most stable sixteen electron complex and hence contains the better π-donating ligand. Finally, frequency calculations have shown that the complex with the better π-donor in the axial plane is indeed a transition state and not a local or global minimum.

Acknowledgment. The financial support of this research by the National Science Foundation (Grant CHE96-15866) and the Robert A. Welch Foundation is greatly appreciated.

Supporting Information Available: X-ray crystallographic files, in CIF format, for the structure determinations of (**2c**, **5c**, **6c**, **7b**, and **8**) are available free of charge via the Internet at http://pubs.acs.org.

IC9804216